Available online at www.sciencedirect.com
ScienceDirect
Ceramics International 37 (2011) 707–713
CERAMICS INTERNATIONAL
www.elsevier.com/locate/ceramint

Structural and electrical properties of $0.56Pb(Ni_{1/3}Nb_{2/3})O_3$–$0.10Pb(Zn_{1/3}Nb_{2/3})O_3$–$0.34PbTiO_3$ ceramics prepared by different ceramic processings

Bijun Fang [a,*], Qingbo Du [a], Dun Wu [a], Limin Zhou [a], Yuejin Shan [b,**], Keitaro Tezuka [b], Hideo Imoto [b]

[a] School of Materials Science and Engineering, Changzhou University, Changzhou, Jiangsu 213164, PR China
[b] Department of Applied Chemistry, Faculty of Engineering, Utsunomiya University, 7-1-2 Yoto, Utsunomiya 321-8585, Japan

Received 22 May 2010; received in revised form 8 July 2010; accepted 26 September 2010
Available online 4 November 2010

Abstract

The ternary system of $0.56Pb(Ni_{1/3}Nb_{2/3})O_3$–$0.10Pb(Zn_{1/3}Nb_{2/3})O_3$–$0.34PbTiO_3$ (0.56PNN–0.10PZN–0.34PT) ceramics were prepared by conventional solid-state reaction method via straight mixed oxide method, columbite precursor method and B-site oxide mixing route. X-ray diffraction (XRD) measurement demonstrated that both the tetragonal and rhombohedral phases coexist in the B-site oxide mixing route prepared ceramics accompanied by the largest content of perovskite phase of 95.18%. The 0.56PNN–0.10PZN–0.34PT ceramics prepared by the straight mixed oxide method and the B-site oxide mixing route exhibit rather homogeneous microstructure. As a comparison, in the columbite precursor method prepared ceramics nebulous granules and octahedral or other polyhedral morphology grains are observed. All the sintered ceramics exhibit diffused ferroelectric phase transition where the dielectric response peaks are broad, diffused and strongly frequency dependent. However, the temperature of dielectric maximum (T_m) increases greatly from 398.0 K of the 0.56PNN–0.10PZN–0.34PT ceramics prepared by the B-site oxide mixing route to 423.3 K of the ones prepared by the straight mixed oxide method. Saturated and symmetric *P–E* hysteresis loops are observed in all the sintered ceramics, where the B-site oxide mixing route prepared ceramics exhibit large value of remanent polarization (P_r) of 17.13 $\mu C/cm^2$ and the least value of coercive field (E_c) of 11.99 kV/cm. Piezoelectric constant (d_{33}) exhibits the largest value of 449 pC/N for the ceramics prepared by the B-site oxide mixing route. Such results are related to the phase composition, density and porosity of the ceramics.

Keywords: C. Electrical properties; Phase transition; Columbite precursor method; B-site oxide mixing route

1. Introduction

A novel methodology to stabilize perovskite phase and develop piezoelectric materials has been conducted by adding stable perovskite structure normal ferroelectrics to relaxor ferroelectrics. The formation of solid solution increases the tolerance factor and electronegativity difference, i.e., ionic bond, and consequently stabilizes the perovskite structure [1]. Ferroelectric ceramics composed of normal and relaxor ferroelectric materials have been reported to exhibit exceptionally excellent dielectric, piezoelectric, electrostrictive and electro-optical properties [2–4]. Among which $(1-x)Pb(Ni_{1/3}Nb_{2/3})O_3$–$xPbTiO_3$ (PNN–PT) is a well known solid solution. PNN–PT exhibits promising applications in low-hysteresis sensor and actuator domains for its excellent dielectric and piezoelectric properties especially with the composition around the morphotropic phase boundary (MPB) [5,6].

MPB has become a popular research subject since the report of $Pb(Zr_xTi_{1-x})O_3$ ferroelectric material because PZT with composition close to the MPB exhibits enhanced microstructure and high dielectric, piezoelectric and ferroelectric properties [7]. MPB is considered as a region connecting two adjacent ferroelectric phases with equivalent energy state and similar structure. The discovery of low symmetry phase around the vicinity of MPB in $Pb(Mg_{1/3}Nb_{2/3})O_3$–$PbTiO_3$ (PMN–PT) and related materials has changed the picture of

* Corresponding author. Tel.: +86 519 86330100; fax: +86 519 86330095.
** Corresponding author. Tel.: +81 28 689 6174; fax: +81 28 689 6174.
E-mail addresses: fangbj@cczu.edu.cn (B. Fang), shan@cc.utsunomiya-u.ac.jp (Y. Shan).

0272-8842/$36.00
doi:10.1016/j.ceramint.2010.09.057

MPB since polarization vector can rotate within a monoclinic plane and complex sequence of phase transition exists in these systems [7–9].

The MPB of PNN–PT is known to locate in the composition range of $x = 0.34$–0.38, which is considered as a region connecting rhombohedral and tetragonal ferroelectric phases [5,6]. Phase pure perovskite PNN–PT ceramics can be prepared by a columbite precursor method but with some difficulty. The columbite precursor method involves two calcination steps, i.e., the formation of columbite precursor $NiNb_2O_6$ and the calcination of $NiNb_2O_6$, PbO and TiO_2 to form perovskite PNN–PT, which was devised by Swartz and Shrout to synthesize stoichiometric perovskite $Pb(Mg_{1/3}Nb_{2/3})O_3$ (PMN) [10]. The columbite precursor method effectively decreases the formation of pyrochlore phase and stabilizes perovskite structure since the direct contact and the intermediate reaction between PbO and Nb_2O_5 can be bypassed [10,11].

Recently, the perovskite phase formation, the character of the successive phase transformation of the structural and electrical properties of the $Pb(Zn_{1/3}Nb_{2/3})O_3$–doped $Pb(Ni_{1/3}Nb_{2/3})O_3$–$PbTiO_3$ (PNN–PZN–PT) pseudo ternary ferroelectric ceramics prepared by conventional solid-state reaction method via the B-site oxide mixing route were reported [12]. In that work, the sintering conditions, the solid-solution content limitation of PZN in the system, the perovskite structure development, and the successive change of the ferroelectric phase transition of the PNN–PZN–PT ceramics were studied systematically. However, perovskite ferroelectrics are sensitive to processing varieties and extremely difficult to fabricate reproducibly without the appearance of pyrochlore phase. Furthermore, the phase transition character and electrical properties of relaxor-based ferroelectrics are greatly influenced by density, microstructural feature, pyrochlore phase distribution, composition and phase, which in turn depend on ceramic processing [13–15]. In the present work, the conventional straight mixed oxide method, the columbite precursor method and the B-site oxide mixing route were used to synthesize $0.56Pb(Ni_{1/3}Nb_{2/3})O_3$–$0.10Pb(Zn_{1/3}Nb_{2/3})O_3$–$0.34PbTiO_3$ (0.56PNN–0.10PZN–0.34PT) ceramics, then the influence of ceramics processing on perovskite phase formation and electrical properties can be researched. This composition was chosen since previous work [12] discovers that such composition locates around the MPB composition in the PNN–PZN–PT system and exhibit excellent electrical properties.

2. Experimental procedure

0.56PNN–0.10PZN–0.34PT ferroelectric ceramics were prepared by the conventional straight mixed oxide method, the columbite precursor method and the B-site oxide mixing route. The conventional straight mixed oxide method utilized a one-step solid-state reaction with all of the starting oxides; the columbite precursor method prepared columbite precursors $NiNb_2O_6$ and $ZnNb_2O_6$, respectively, at initial step followed by a reaction with PbO and TiO_2 to form ternary 0.56PNN–0.10PZN–0.34PT at second step; and the B-site oxide mixing technique was a modification of the columbite precursor method, where all oxides of the B-site of the perovskite structure were pre-calcined together simultaneously instead of preparing different columbite precursors separately and then the synthesized B-site precursor reacted with PbO to form perovskite 0.56PNN–0.10PZN–0.34PT [11,14]. The content of PZN was chosen as 10 mol% since preliminary experiment confirmed that pyrochlore phase increases sharply when the content of PZN exceeds 10 mol% in the PNN–PZN–PT system.

High-purity oxides, PbO (>99.9%), NiO (99.9%), ZnO (>99.95%), Nb_2O_5 (>99.9%) and TiO_2 (>99.9%) were used as raw materials. In order to obtain stoichiometric composition, the raw oxides were separately dried before weighing and the synthesized columbite precursors and the B-site precursors were weighed and introduced into the batch calculation. Detailed synthesis procedure of the 0.56PNN–0.10PZN–0.34PT ceramics is shown in Table 1.

During the ceramic processing, stoichiometric oxides were weighed in each step according to the chemical composition of 0.56PNN–0.10PZN–0.34PT. The calcined powders were cold isostatically pressed into pellets at a pressure of 400 kgf/cm^2 with the addition of 1 wt% polyvinyl alcohol (PVA) binder and sintered at 1185 °C for 2 h. The pellets were buried under an equiweight mixture of raw oxides with the same composition in a covered crucible to minimize the evaporation of lead during sintering. In all the above three methods no excess of PbO was added for the preparation of 0.56PNN–0.10PZN–0.34PT ceramics.

The sintered ceramics were ground and polished to obtain flat and parallel surfaces. The perovskite phase formation and the amount of pyrochlore phase of the calcined powders and the sintered ceramics were analyzed by X-ray diffraction measurement (XRD, Rigaku RINT-2200VS Diffractometer). The amount of perovskite phase can be calculated using an

Table 1
Synthesis conditions of the fabrication of the 0.56PNN–0.10PZN–0.34PT ceramics by the three methods.

Procedure	Straight mixed oxide method	Columbite precursor method	B-site oxide mixing route
Precursor synthesis	–	$NiO + Nb_2O_5 \xrightarrow[\text{calcine } 4\text{ h}]{1000\ ^\circ C} NiNb_2O_6$ $ZnO + Nb_2O_5 \xrightarrow[\text{calcine } 4\text{ h}]{1000\ ^\circ C} ZnNb_2O_6$	NiO, ZnO, Nb_2O_5, TiO_2 pre-calcine at 1000 °C for 4 h
Calcine	All oxides calcine at 925 °C for 2 h	$NiNb_2O_6$, $ZnNb_2O_6$, PbO, TiO_2 calcine at 925 °C for 2 h	B-site precursor, PbO calcine at 925 °C for 2 h
Sinter		Sinter at 1185 °C for 2 h	

approximate method:

$$\% \text{ Perovskite} = \frac{I_{perov} \times 100}{I_{perov} + I_{pyro}}$$

where the concentration of perovskite and pyrochlore phases was determined by the relative intensity of the (1 1 0) perovskite peak (I_{perov}) and the (2 2 2) pyrochlore peak (I_{pyro}) [15]. Microstructure of the sintered ceramics was observed by scanning electron microscopy (SEM, JSM6360LA) using free surfaces of the specimens. For electrical properties characterization, silver paste was coated on both surfaces of the well-polished pellets and fired at 650 °C for 15 min to provide robust electrodes. The ceramics were poled for piezoelectric measurement at an electric field of 2.5 kV/mm in silicon oil at 120 °C for 15 min and then slowly cooled down to room temperature while maintaining half of the applied electric field. Detailed measurement procedures were described elsewhere [16].

3. Results and discussion

Important technological problems associating with the processing of lead-containing perovskites are the control of evaporation of PbO and the inhibition of formation of pyrochlore phase during sintering, which depends mainly on raw materials, sintering conditions and ceramic processing. Fig. 1 shows XRD patterns of the 0.56PNN–0.10PZN–0.34PT ceramics prepared by the above three methods. Main phase of perovskite is obtained by the three methods. However, due to the metastability of perovskite PZN, $Pb_3Nb_4O_{13}$-type pyrochlore phase appears in all the sintered ceramics. The content of pyrochlore phase exhibits great dependence on ceramic processing, which is shown in Table 2 estimated based on XRD results. The efficiency and feasibility of the B-site oxide mixing route in the synthesizing of complex perovskite ferroelectrics is proven again since the content of pyrochlore phase is the least, 4.82%, of all the sintered 0.56PNN–0.10PZN–0.34PT ceramics. The success of the B-site oxide mixing route in suppressing pyrochlore phases can be attributed to the intermediate compounds formed during pre-calcining [11,14,15]. No trace of Nb_2O_5 retains in the B-site oxide mixing route precursors, which bypasses the preferential reaction of Nb_2O_5 with PbO to form stable pyrochlore phase.

Table 2
The content of perovskite phase, bulk density and room-temperature dielectric property measured at 1 kHz of the 0.56PNN–0.10PZN–0.34PT ceramics prepared by the three methods.

Ceramic processing	Percentage of perovskite phase	Bulk density (g/cm^3)	Dielectric constant	Dielectric loss
Straight mixed oxide method	83.73	7.9053	1783	0.02961
Columbite precursor method	94.30	7.7858	2192	0.03053
B-site oxide mixing route	95.18	7.8406	2259	0.03497

XRD patterns of the 0.56PNN–0.10PZN–0.34PT ceramics over the diffraction degree range $2\theta = 43–48^\circ$ are shown in Fig. 2. Multi diffraction peaks appear in the 0.56PNN–0.10PZN–0.34PT ceramics prepared by the B-site oxide mixing route due to the superposition of the rhombohedral and tetragonal {2 0 0} diffraction peaks. The single diffraction peak of (2 0 0) reflection indicates that the 0.56PNN–0.10PZN–0.34PT ceramics prepared by the straight mixed oxide method exist in rhombohedral phase. Strong splitting of the (2 0 0) diffraction peak indicates that the columbite precursor method prepared samples are tetragonal phase. As a comparison, the tetragonal and rhombohedral phases coexist in the B-site oxide mixing route prepared samples due to the coexistence of the (2 0 0) tetragonal and (2 0 0) rhombohedral plane. The compositions of the tetragonal and rhombohedral phases can be estimated by integral area of corresponding diffraction peaks.

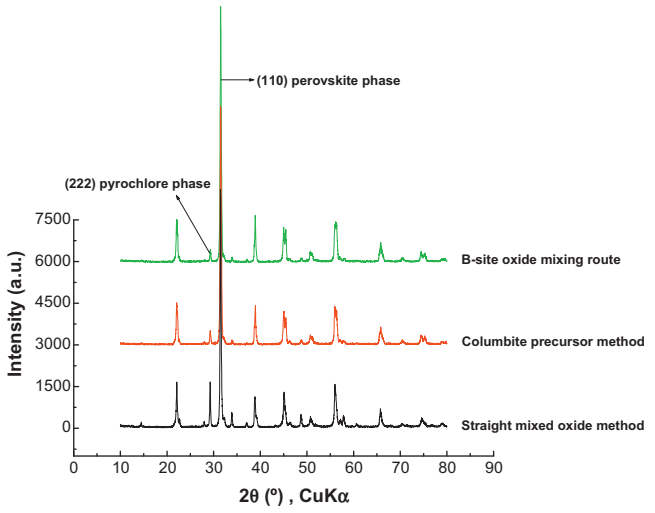

Fig. 1. XRD patterns of the 0.56PNN–0.10PZN–0.34PT ceramics prepared by the three methods.

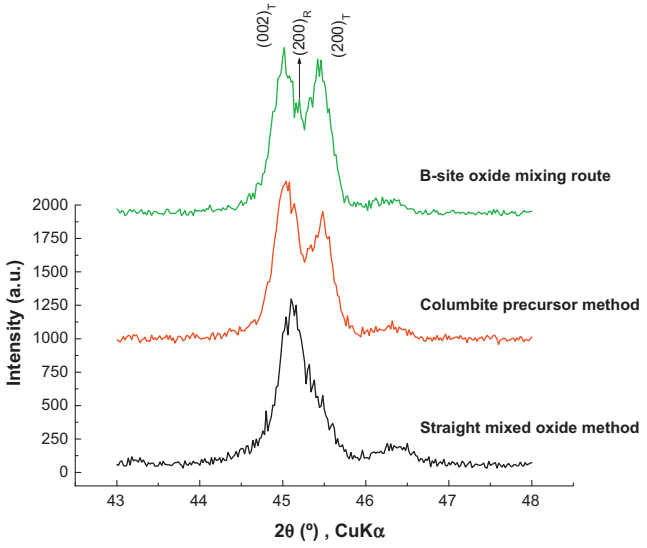

Fig. 2. XRD patterns of the ⟨2 0 0⟩ diffraction peaks of the 0.56PNN–0.10PZN–0.34PT ceramics prepared by the three methods.

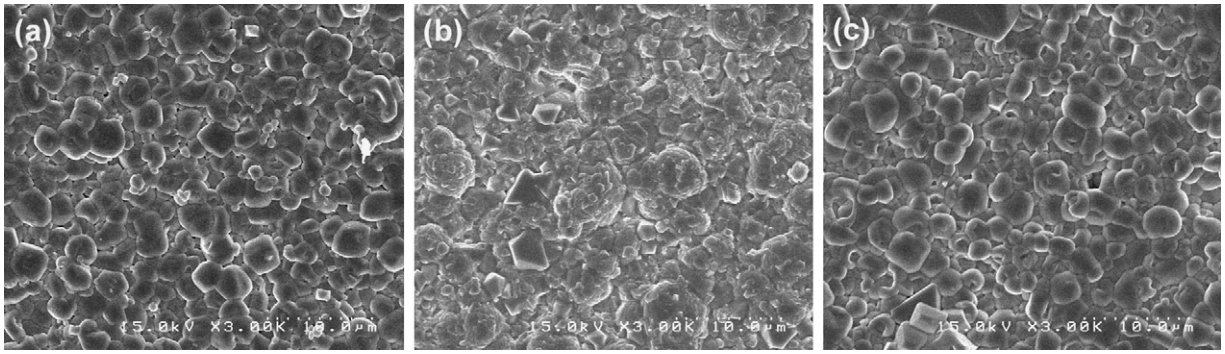

Fig. 3. SEM photographs of free surfaces of the 0.56PNN–0.10PZN–0.34PT ceramics prepared by the three methods. The ceramics were thermal etched at 825 °C for 30 min before SEM observation. (a) Straight mixed oxide method; (b) columbite precursor method; (c) B-site oxide mixing route.

SEM images of the 0.56PNN–0.10PZN–0.34PT ceramics prepared by different methods are shown in Fig. 3. The 0.56PNN–0.10PZN–0.34PT ceramics prepared by the straight mixed oxide method and the B-site oxide mixing route exhibit rather homogeneous microstructure. The content of enclosed porosity observed in the SEM micrographs is consistent with the density results, where the ceramic bulk density is 7.9053 and 7.8406 g/cm^3 for the straight mixed oxide method and the B-site oxide mixing route, respectively. Slight quantity of small granules and scraps congregated in grain conjunctures and attached on grain surface may be pyrochlore phase and glass phase introduced during the processing of samples for SEM observation. Liquid-phase sintering mechanism may take partial effect in the densification of these ceramics due to the round grain morphology [17]. As a comparison, nebulous granules and octahedral or other polyhedral morphology grains appear in the columbite precursor method prepared samples. Therefore, different ceramic processing produces ceramics with different densification, grain size and density, which will exert great influence on electrical properties of ceramics.

In strong polarized dielectrics, the orientation of dipoles facilitates with the increase of temperature. Therefore, dielectric constant exhibit great dependence on two variable factors, i.e., temperature and frequency. Temperature dependence of relative dielectric constant of the 0.56PNN–0.10PZN–0.34PT ceramics prepared by different methods is shown in Fig. 4. At room temperature, the B-site oxide mixing route prepared samples exhibit the largest value of relative dielectric constant and dielectric loss tangent. The dielectric anomalies appeared at different temperatures can be attributed to the phase transition from rhombohedral/tetragonal ferroelectric (FE) phase to cubic paraelectric (PE) phase. Apparent frequency dispersion around a large temperature range is observed for all the samples prepared by the three methods, where the dielectric response peaks are broad, diffused and strongly frequency dependent. The temperature of dielectric maximum (T_m) changes greatly with the increase of frequency and the full-width-at-half maximum (FWHM) of the dielectric peaks is around 75 K, which shows the nature character of relaxor ferroelectrics. However, T_m shifts towards lower temperature with the increase of frequency, which is beyond our comprehension since T_m increases with the increase of frequency in typical relaxor ferroelectrics [18].

Fig. 5 shows a comparison of dielectric property of the 0.56PNN–0.10PZN–0.34PT ceramics prepared by different methods. The effects of ceramic processing on dielectric

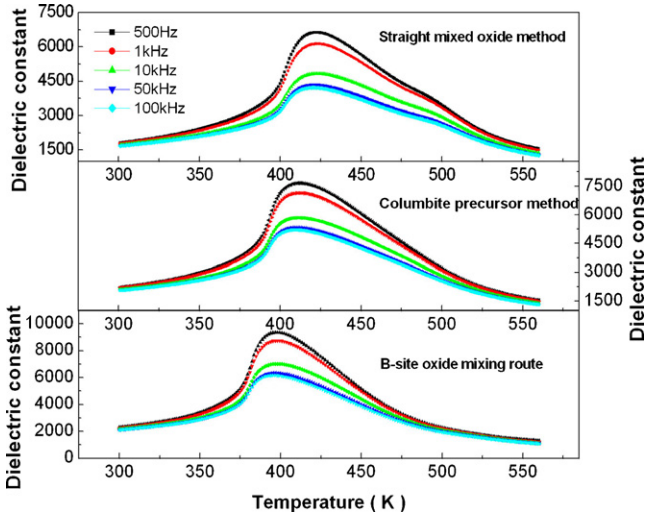

Fig. 4. Temperature dependence of relative dielectric constant of the 0.56PNN–0.10PZN–0.34PT ceramics prepared by the three methods measured at several frequencies upon heating.

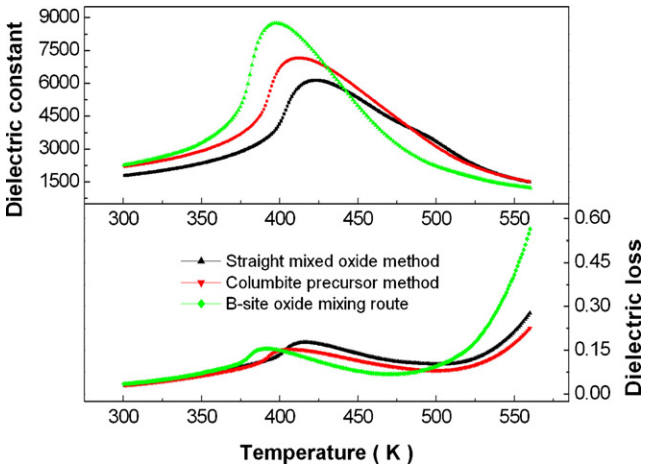

Fig. 5. Temperature dependence of dielectric constant and loss tangent of the 0.56PNN–0.10PZN–0.34PT ceramics prepared by the three methods measured at 1 kHz upon heating.

Table 3
Comparison of dielectric property of the 0.56PNN–0.10PZN–0.34PT ceramics prepared by the three methods using 1 kHz data.

Ceramic processing	T_{max} (K)	ε_{max}	tan δ_{max}	ΔT (K) 500 Hz–100 kHz	n	C' ($\times 10^6$)	δ (K)
Straight mixed oxide method	423.3	6132	0.1769 (416.3 K)	−2.5	1.8047	15.800	52.880
Columbite precursor method	412.3	7146	0.1539 (406.8 K)	−2.0	1.9199	29.174	52.968
B-site oxide mixing route	398.0	8741	0.1557 (391.3 K)	−2.7	1.8585	17.081	40.622

behavior are shown clearly, which is summarized in Table 3. The B-site oxide mixing route prepared samples exhibit relatively larger value of dielectric constant and narrower dielectric peak at the FE transition temperature (T_m) of 398.0 K with dielectric maximum of 8741 as compared to the samples prepared by the other two methods. The B-site oxide mixing route exhibits superiority in improving dielectric properties. However, T_m increases greatly from 398.0 K of the 0.56PNN–0.10PZN–0.34PT ceramics prepared by the B-site oxide mixing route to 423.3 K of the ceramics of the same composition prepared by the straight mixed oxide method, which cannot be elucidated now.

Dielectric behavior of relaxor-based ferroelectrics can be described by a quadratic law,

$$\frac{1}{\varepsilon} = \frac{1}{\varepsilon_{max}} + \frac{(T - T_{max})^n}{C'}$$

where n is a diffuseness index and C' is a constant [19]. The diffuseness index can be solved graphically from the graphs of $\ln(1/\varepsilon - 1/\varepsilon_m)$ versus $\ln(T - T_{max})$, which is shown in Fig. 6. The slope of the curve represents the value of the diffuseness index, and the intercept gives the diffuseness parameter by equation:

$$\delta = \left(\frac{e^{-\text{intercept}}}{2\varepsilon_{max}}\right)^{1/n}$$

The values of the parameters obtained by a linear regression analysis of the data shown in Fig. 6 are also listed in Table 3. The columbite precursor method prepared samples exhibit the largest value of diffuseness index n of 1.9199, whereas the B-site oxide mixing route prepared samples exhibit the least value of diffuseness parameter δ of 40.622. Such variation is considered as correlating with the inhomogeneity at atomic scale of the 0.56PNN–0.10PZN–0.34PT ceramics prepared by different methods.

Dielectric properties at cryogenic temperatures of the 0.56PNN–0.10PZN–0.34PT ceramics prepared by different methods are shown in Fig. 7. At low temperature, dielectric frequency dispersion is suppressed greatly for all the ceramics synthesized by the three methods. For all the 0.56PNN–0.10PZN–0.34PT ceramics prepared by the three methods a dielectric shoulder appears around 98.7 K accompanied by the appearance of dielectric loss peaks at lower temperature around 46 K, which may be attributed to an unknown structural phase transition or the formation of ferroelectric domain with lower symmetry. Low-temperature XRD measurements are needed to provide insight into the nature of this possible structural phase transition.

P–E hysteresis loops at room temperature of the B-site oxide mixing route prepared 0.56PNN–0.10PZN–0.34PT ceramics with different electric field are shown in Fig. 8. With the increase of electric field strength, the shape of hysteresis loop develops from a nearly linear relationship at 5 kV/cm to a nonlinear and fully developed symmetric *P–E* loop at 30 kV/cm. In all electric field strength, no apparent evidence of pinning effect or asymmetric loop is observed. Therefore, the electric field strength of 25 kV/cm can afford enough energy to align all domains in the direction of the electric field.

Ferroelectric hysteresis loops of the 0.56PNN–0.10PZN–0.34PT ceramics prepared by different methods are shown in

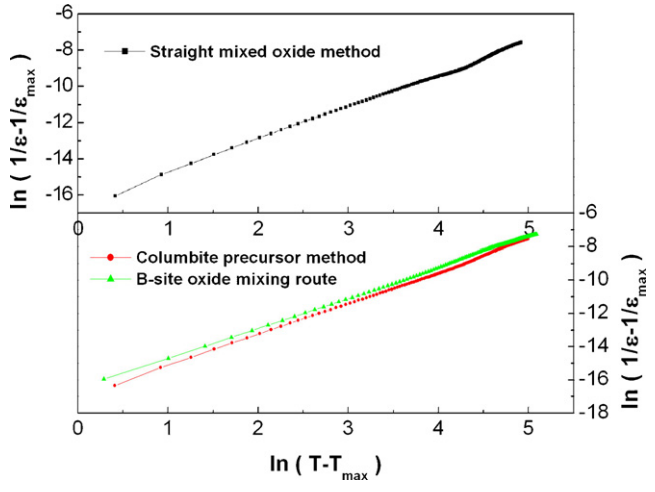

Fig. 6. Plot of $\ln(1/\varepsilon - 1/\varepsilon_m)$ versus $\ln(T - T_{max})$ of the 0.56PNN–0.10PZN–0.34PT ceramics prepared by the three methods using 1 kHz data.

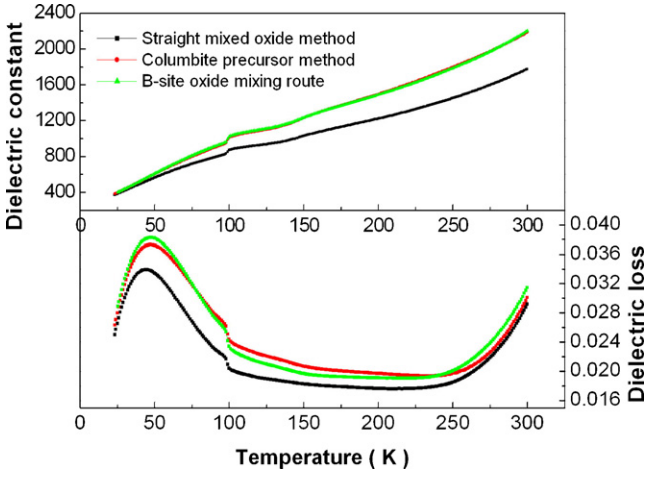

Fig. 7. Temperature dependence of dielectric constant and loss tangent of the 0.56PNN–0.10PZN–0.34PT ceramics prepared by the three methods measured at 1 kHz upon heating at cryogenic temperatures.

Table 4
Ferroelectric and piezoelectric (symmetrical selection of measurement points within round specimens) properties of the 0.56PNN–0.10PZN–0.34PT ceramics prepared by different methods measured at room temperature.

Ceramic processing	Straight mixed oxide method				Columbite precursor method				B-site oxide mixing route			
P_r (μC/cm^2)	13.78				17.39				17.13			
E_c (kV/cm)	13.65				13.10				11.99			
d_{33} (pC/N)	367	360	364	360	417	419	408	420	443	433	450	457
	350	364	372	373	417	431	414	401	440	445	446	462
	360	382	369	367	430	431	405	401	449	443	468	448
d_{33} (pC/N, mean value)	366				416				449			

Fig. 9. With the electric field strength of 25 kV/cm, the polarization loops of all the ceramics are well developed showing large remanent polarization (P_r). All the hysteresis loops exhibit typical ''square'' form, which is characteristic of a ferroelectric microdomain state where long-range cooperation exists between dipoles. The values of P_r and coercive field (E_c) are determined based on the saturated P–E loops, which is shown in Table 4. The straight mixed oxide method prepared ceramics exhibit the largest value of E_c 13.65 kV/cm, whereas the columbite precursor method prepared ceramics possess the largest value of P_r 17.39 μC/cm^2. The value of P_r of the B-site oxide mixing route prepared ceramics can be comparable to those of the columbite precursor method prepared ones, whereas the value of E_c is the least of 11.99 kV/cm in all the synthesized ceramics. The variation of the values of P_r and E_c is correlated with the content of rhombohedral phase and porosity effect in the sintered ceramics.

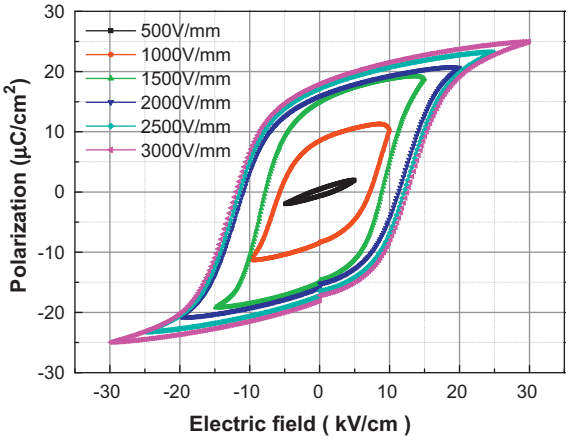

Fig. 8. P–E hysteresis loops of the 0.56PNN–0.10PZN–0.34PT ceramics prepared by the B-site oxide mixing route measured at room temperature with different electric field.

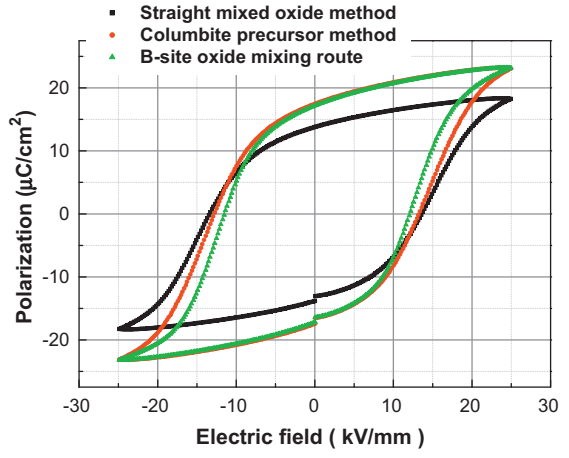

Fig. 9. P–E hysteresis loops of the 0.56PNN–0.10PZN–0.34PT ceramics prepared by different methods measured at 25 kV/cm.

Piezoelectric property measured at the same condition of the 0.56PNN–0.10PZN–0.34PT ceramics prepared by different methods is shown in Table 4. The values of piezoelectric constant d_{33} of all the sintered ceramics varies within a pellet, which is an ordinary phenomenon in ferroelectrics. Such variation can be attributed the inhomogeneity of composition and/or the existence of micropolar regions. The B-site oxide mixing route prepared ceramics exhibit the largest value of d_{33} of 449 pC/N, the columbite precursor method prepared ceramics has a larger value of d_{33} of 416 pC/N, whereas the straight mixed oxide method prepared ceramics exhibit the least value of d_{33} of 366 pC/N. These d_{33} values are relatively larger compared to those reported in literature of similar system. The largest d_{33} value of the B-site oxide mixing route prepared ceramics is likely due to the relatively larger bulk density, relatively lower porosity and the least content of pyrochlore phase.

4. Conclusions

Phase transition behavior and electrical properties of the 0.56PNN–0.10PZN–0.34PT ceramics prepared by the straight mixed oxide method, columbite precursor method and B-site oxide mixing route were investigated. Tetragonal and rhombohedral phases coexist in the B-site oxide mixing route prepared 0.56PNN–0.10PZN–0.34PT ceramics accompanied by relatively higher bulk density and rather homogeneous microstructure. Diffused ferroelectric phase transition is observed for all the ceramics synthesized whereas T_m increases greatly from 398.0 K of the B-site oxide mixing route prepared ones to 423.3 K of the straight mixed oxide method prepared ones of the same composition. The B-site oxide mixing route prepared ceramics exhibit large P_r value of 17.13 μC/cm^2, the least E_c value of 11.99 kV/cm and the largest d_{33} value of 449 pC/N. These results can be attributed the phase composition, density and porosity effect of the ceramics prepared by different ceramic processing.

Acknowledgments

The authors thank the Scientific Research Foundation for the Returned Overseas Chinese Scholars, State Education Ministry, the International Scientific Cooperation Project of Changzhou Scientific Bureau (Grant No. CZ2008014) and the Natural Science Fundamental Research Project of Jiangsu Colleges and Universities (Grant No. 08KJB430001) for financial support.

References

[1] T.R. Shrout, A. Halliyal, Preparation of lead-based ferroelectric relaxors for capacitors, Am. Ceram. Soc. Bull. 66 (1987) 704.
[2] X. Wen, C. Feng, L. Chen, S. Huang, Dielectric tunability and imprint effect in $Pb(Mg_{1/3}Nb_{2/3})O_3$–$PbTiO_3$ ceramics, Ceram. Int. 33 (2007) 815.
[3] Y. Chen, J. Zhu, D. Xiao, B. Qin, Y. Jiang, Bismuth-modified $BiScO_3$–$PbTiO_3$ piezoelectric ceramics with high Curie temperature, Mater. Lett. 62 (2008) 3567.
[4] E.F. Alberta, A.S. Bhalla, Low-temperature property investigation of the lead indium–niobate–lead nickel–niobate solid solution, J. Phys. Chem. Solids 63 (2002) 1759.
[5] P.-H. Xiang, N. Zhong, X.-L. Dong, Single-calcination synthesis of pyrochlore-free $Pb(Ni_{1/3}Nb_{2/3})O_3$–$PbTiO_3$ using a coating method, Solid State Commun. 127 (2003) 699.
[6] C. Lei, K. Chen, X. Zhang, Dielectric and ferroelectric properties of $Pb(Ni_{1/3}Nb_{2/3})O_3$–$PbTiO_3$ ferroelectric ceramic near the morphotropic phase boundary, Mater. Lett. 54 (2002) 8.
[7] B. Noheda, J.A. Gonzalo, L.E. Cross, R. Guo, S.-E. Park, D.E. Cox, G. Shirane, Tetragonal-to-monoclinic phase transition in a ferroelectric perovskite: the structure of $PbZr_{0.52}Ti_{0.48}O_3$, Phys. Rev. B 61 (2000) 8687.
[8] Z.-G. Ye, B. Noheda, M. Dong, D. Cox, G. Shirane, Monoclinic phase in the relaxor-based piezoelectric ferroelectric $PbMg_{1/3}Nb_{2/3}O_3$–$PbTiO_3$ system, Phys. Rev. B 64 (2001) 184114.
[9] R. Haumont, B. Dkhil, J.M. Kiat, A. Al-Barakaty, H. Dammak, L. Bellaiche, Cationic-competition-induced monoclinic phase in high piezoelectric $(PbSc_{1/2}Nb_{1/2}O_3)_{1-x}$–$(PbTiO_3)_3$ compounds, Phys. Rev. B 68 (2003) 014114.
[10] S.L. Swartz, T.R. Shrout, Fabrication of perovskite lead magnesium niobate, Mater. Res. Bull. 17 (1982) 1245.
[11] J.-S. Pan, X.-W. Zhang, Structural phase-transition region and electrical properties of $Pb(Ni_{1/3}Nb_{2/3})O_3$–$Pb(Ni_{1/3}Nb_{2/3})O_3$–$PbTiO_3$ ceramics, J. Appl. Phys. 99 (2006) 034106.
[12] B. Fang, R. Sun, Y. Shan, K. Tezuka, H. Imoto, Phase transition, structural and electrical properties of $Pb(Zn_{1/3}Nb_{2/3})O_3$-doped $Pb(Ni_{1/3}Nb_{2/3})O_3$–$PbTiO_3$ ceramics prepared by solid-state reaction method, J. Phys. Chem. Solids 70 (2009) 893.
[13] G. Rujijanagul, N. Vittayakorn, Influence of fabrication processing on phase transition and electrical properties of $0.8Pb(Zr_{1/2}Ti_{1/2})O_3$–$0.2Pb(Ni_{1/3}Nb_{2/3})O_3$ ceramics, Curr. Appl. Phys. 8 (2008) 88.
[14] M. Orita, H. Satoh, K. Aizawa, K. Ametani, Preparation of ferroelectric relaxor $Pb(Zn_{1/3}Nb_{2/3})O_3$–$Pb(Mg_{1/3}Nb_{2/3})O_3$–$PbTiO_3$ by two-step calcination method, Jpn. J. Appl. Phys., Part 1 31 (1992) 3261.
[15] R.M.V. Rao, A. Halliyal, A.M. Umarji, Perovskite phase formation in the relaxor system $[Pb(Fe_{1/2}Nb_{1/2})O_3]_{1-x}$–$[Pb(Zn_{1/2}Nb_{1/2})O_3]_x$, J. Am. Ceram. Soc. 79 (1996) 257.
[16] B. Fang, Z. Cheng, R. Sun, C. Ding, Preparation and electrical properties of $(1-x)Sr(Fe_{1/2}Nb_{1/2})O_3$–$xPbTiO_3$ ferroelectric ceramics, J. Alloys Compd. 471 (2009) 539.
[17] S.-J. Park, H.-Y. Park, K.-H. Cho, S. Nahm, H.-G. Lee, D.-H. Kim, B.-H. Choi, Effect of CuO on the sintering temperature and piezoelectric properties of lead-free $0.95(Na_{0.5}K_{0.5})NbO_3$–$0.05CaTiO_3$ ceramics, Mater. Res. Bull. 43 (2008) 3580.
[18] Z.-G. Ye, Relaxor ferroelectric complex perovskites: structure, properties and phase transitions, Key Eng. Mater. 155–156 (1998) 81.
[19] K. Uchino, S. Nomura, Critical exponents of the dielectric constants in diffused-phase-transition crystals, Ferroelectr. Lett. 44 (1982) 55.